

Preparation of solvent resistant supports through formation of a semi-interpenetrating polysulfone/ polyacrylate network using UV cross-linking – Part 1: selection of optimal UV curing conditions

Peter-Renaat Van den Mooter^{a,1}, Nick Daems^{a,b,1}, Ivo F. J. Vankelecom^{a,*}

^a Centre for Surface Chemistry and Catalysis, KU Leuven, Celestijnenlaan 200F, Box 2461, 3000 Heverlee, Belgium

^b Advanced Reactor Technology , U Antwerpen, Campus Drie Eiken, Universiteitsplein 1, 2610 Wilrijk, Belgium

* Corresponding author. E-mail address: ivo.vankelecom@kuleuven.be (I.F.J. Vankelecom); Tel.: +3216321594

¹ Equal contribution

Abstract

As the number of membrane applications in industrial processes keeps increasing, more and more attention is being paid to their physical and chemical stability. Especially during cleaning procedures and under actual operation conditions the lack of a sufficient stability still remains an issue thereby seriously limiting the membrane lifetime and increasing the operating cost. Currently, different methods are applied during the synthesis to improve the stability of polymeric membranes. One promising method to produce solvent resistant membranes (in this specific case supports) is by cross-linking polymeric membranes via photo-irradiation. In this study, three different UV curing conditions (e.g. UV – spark, UV – microwave and UV – LED) were studied in depth by evaluating the cross-linker conversion degree with infra-red spectroscopy. Ultimately the 365 nm UV-LED light was selected as the most optimal UV curing condition. This unit is further used to study the optimal compositional and non-compositional parameters to produce solvent resistant supports in a continuous membrane casting line for up-scaling.

Keywords: Photo-irradiation; UV Cross-linking; Sartomer; Upscaling; PSU

No conflicts of interest.

1. Introduction

Membrane technology is an established separation technology, e.g. in water treatment, food processing and gas separation [1–8]. Because of their well-known economic and environmental advantages, such as a high energy efficiency and a limited waste production, membranes are widely considered as attractive alternatives for conventional technologies, like e.g. distillation, crystallization or extractions. Furthermore, upscaling membranes and integrating them into existing industrial processes is relatively straightforward. Membrane technology is therefore considered as a key technology for process intensification. However, membranes often still suffer from a limited chemical stability, especially during actual industrial processes or membrane cleaning processes. One method to improve the chemical stability of a polymeric membrane is to cross-link the polymer chains [9–11]. Cross-linking can be achieved e.g. by means of a thermal treatment [12–14], chemical reactions [15–19] or photo-irradiation using IR- [20,21] or UV-sources [22–26].

This study focuses on the latter, which makes use of photo-irradiation to tune the properties of polymeric membranes [26–28]. By selective excitation with UV-irradiation, free radicals are generated through UV absorption [29]. It is an easy and versatile method to synthesize cross-linked membranes. The first step is the preparation of a homogeneous casting solution, including the selected polymer, a photo-initiator, a cross-linker and a solvent. At lab-scale, this solution is then cast onto a glass-plate or a supporting membrane, resulting in a UV-curable membrane after solidification. This solidification normally takes place via the process of phase inversion [30]. A critical aspect of this synthesis process is the choice of a suitable photo-initiator and cross-linker type. The photo-initiator has to be chosen such that (1) it can produce radicals in the available light spectrum, and (2) ensures penetration of the UV light throughout the whole thickness of the cast layer. The latter is quite challenging as the membranes are generally opaque after solidification and relatively thick to ensure good mechanical strength. Additionally, the choice of the cross-linker also influences the UV curing efficiency, as their functional groups and water affinity (of importance during the phase inversion process) can have a major impact on the resulting cross-linking degree [22].

The aim of this work is the synthesis of solvent-resistant support layers for a broad range of potential large-scale applications (e.g. in food industry, gas separation,...). Three different UV

light sources (i.e. UV - spark, UV - microwave and UV - LED) were tested to photo-cure a standard polysulfone (PSU) - based membrane prepared via phase inversion. Conversion of the functional groups for cross-linking (i.e. double bonds) and ease of operation are key parameters to select the optimal UV curing technique and unit for our purpose. The best unit will be used in future studies to install a continuous upscaled membrane casting line.

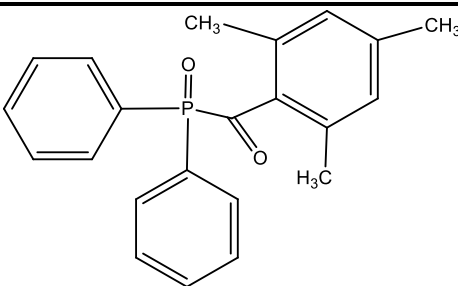
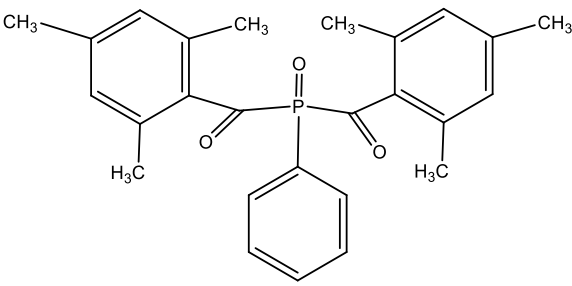
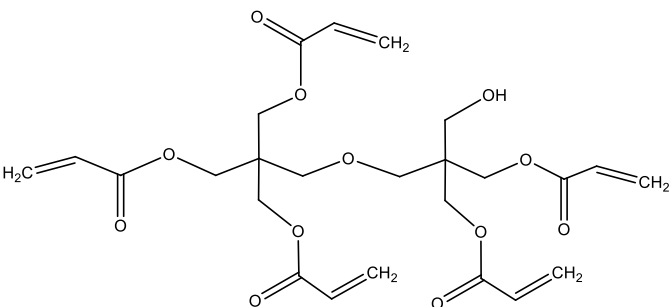
2. Experimental

2.1. Materials

2.1.1. Reagents

Commercial PSU (Udel[®] P-1700 LCD, $M_n \sim 21,000 \text{ g mol}^{-1}$) was supplied by Solvay and dried in an oven for 24 h at 100 °C prior to use. Photo-initiators, 2,4,6-trimethylbenzoyl-diphenylphosphineoxide (TPO) and bis(2,4,6-trimethylbenzoyl)-phenylphosphineoxide (IR819) (Table 1), were obtained from Sigma-Aldrich (Belgium) and TCI Europe NV (Belgium), respectively. The cross-linker dipentaerythritol penta-acrylate (SR399LV) (Table 1) was obtained from Sigma-Aldrich (Belgium). N,N-dimethylformamide (DMF) (99.8 % VWR BDH Prolabo) and tetrahydrofuran (THF) (anhydrous, containing 250 ppm BHT as inhibitor, ≥ 99.9 %, Sigma-Aldrich) were used without further purifications.

Table 1. Chemical structure of photo-initiators and cross-linkers applied in this study.

Compound	Name	Structure
TPO	2,4,6-trimethylbenzoyl-diphenylphosphineoxide (Darocur™ TPO)	
IR819	bis(2,4,6-trimethylbenzoyl)-phenylphospineoxide (Irgacure™ 819)	
SR399LV	Dipentaerythritol penta-acrylate (Sartomer™ SR399 LV)	

2.2. Membrane synthesis and UV cross-linking

To select the optimal UV curing conditions, a standard asymmetric, polymeric membrane was synthesized from PSU via non-solvent induced phase separation (NIPS) [30] (Figure 1), where a solid porous matrix was made via immersion precipitation of a polymer solution in a non-solvent bath. A viscous solution (with a DMF/THF ratio of 85/15) of 21 wt% PSU in DMF was stirred at 80 °C for 3 h until a homogeneous mixture was obtained. After cooling down, 5 wt% of cross-linker, 3 wt% of a photo-initiator and THF, as volatile co-solvent, were added. The solution was then covered in aluminum foil and stirred until complete dissolution. Afterwards, the mixture was left in the fume hood overnight for degassing. Next, the polymer solution was cast with a wet thickness of 200 µm on a glass plate at a speed of 1.29 m/min using an automated casting knife (Braive Instruments, Belgium). Before immersion in the coagulation (i.e. water) bath, the cast film

was left to evaporate for 30 s to create a thin denser top layer. Afterwards, it was stored in the dark in deionized water until UV curing. All steps were performed in the dark, at room temperature and under ambient atmosphere, since no influence of oxygen was observed. The coagulation bath temperature was 18 °C. Membrane strips were then cut into 15 x 45 mm samples and dipped dry with tissue paper before passing them through a UV curing unit.

UV cross-linking was performed under ambient atmosphere using three different UV curing units each having a specific wavelength (range). A parameter screening (e.g. irradiation time, energy dose, frequency, UV lamp intensity) was done for each unit in search for the highest achievable conversion degree of the membrane. After UV curing, the samples were kept in aluminum foil until physicochemical characterization.

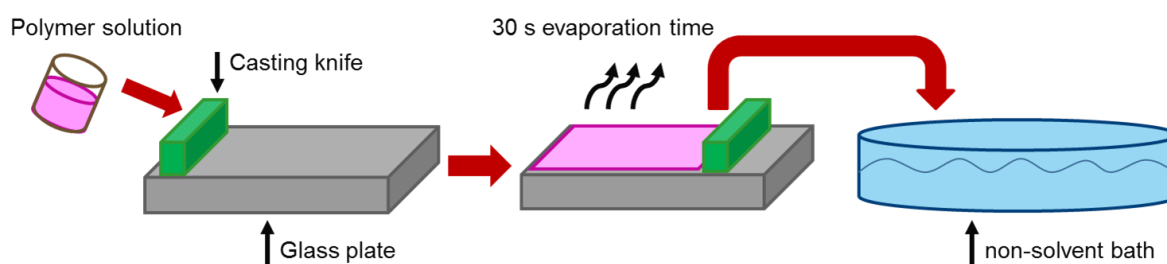


Figure 1. Non-solvent induced phase separation (NIPS).

2.2.1. UV cross-linking units

2.2.1.1. UV - high energy pulsed light

UV - high energy pulsed light, or here referred to as UV - spark, uses high power light pulses emitted by inert-gas flash lamps. It produces large amounts of energy, up to 1 MW, while generating very little heat. Because of its high energy density, the pulsed light can thus penetrate thick and opaque substrates.

The pilot-scale UV system under investigation here, consists of a S-2200 power supply with lamp housing LH-840 and Blitzlamp Type B (Polytec GmbH, DE). The lamp itself has an ozone-free flash tube with Germisil glass envelope that emits a pulse of light with a broad spectrum range of 190 to 1100 nm, as shown in Figure S1 (i.e. visible and UV light) [31,32]. A single pulse of light has a peak output of 0.38 MW, which corresponds to a power of 13 J during 13 μ s. These values are the minimal values that can be set per pulse. Depending on the type of application, these parameters can be changed within a certain range, as shown in Table 2.

Table 2. Parameters of the UV – spark unit.

Parameter	Description	Range
Voltage	Remains constant throughout the pulse sequence	0 to 3000 V
Repetitions	Sets the number of times a sequence will be repeated	0 to 100 Set 0 for continuous operation
Pulse Mode	Sets the pulse mode and determines the limits for certain parameters	Short (S) or Micro (M)
Frequency	Sets the rate at which the sequence will repeat in micro (M) mode	1 to 1000 Limited by factory-set power limits
Duration	Time of pulse	50 to 5000 μ s
Delay	When in Short (S) mode, value measured in milliseconds (ms); in Micro (M) mode, in microseconds (μ s)	(S) 50 to 3000 ms (M) 50 – 50,000 μ s

2.2.1.2. UV – microwave powered electrodeless lamp

A UV – microwave powered electrodeless lamp, here abbreviated as UV – microwave, uses a tubular electrodeless bulb in an elliptical reflector that focuses an intense strip of UV energy onto the substrate.

In this study, a pilot-scale UV system consisting of an ISA carbon filter stand, a L110 conveyor belt and a F300S lamp housing (UVio Ltd, UK), was applied. In the F300S housing, a Light Hammer 6 D-bulb lamp (13mm) was installed with irradiation light within the UVA range (320 – 390 nm) and total spectrum range, as shown in Figure S2 [33]. The parameters that can be altered in this setup are the conveyor belt speed, lamp intensity and duration.

2.2.1.3. UV - light emitting diode

UV – light emitting diode uses the LED technology for generating UV light with a specific wavelength, i.e. holes and electrons on the interface of two semiconductor materials are combined, which creates UV light [34,35].

In this study, a pilot-scale UV LED system OmniCure® - AC8300 (Polytec GmbH, DE) is used. The lamp had a specific wavelength of 365 nm and a typical peak irradiance of 2 W/cm² at 2.0 mm of the substrate (Figure S3) [36]. The parameters controlled here were peak power, frequency and duration.

2.3. Chemical characterization

2.3.1. ATR-FTIR

The acrylate curing efficiency was determined as the conversion of the acrylate double bonds to single bonds and was monitored by an Attenuated Total Reflectance – Fourier Transform Infrared Spectroscopy (ATR-FTIR) spectrometer (VARIAN 620 IR FT-IR Imaging Microscope) using a Germanium Slide PN 066-4903 ATR crystal with a resolution of 4 cm⁻¹ [37]. The top of each membrane sample was scanned for 64 times between 4000 and 400 cm⁻¹. The conversion efficiency was then calculated by the ratio between UV cured and non-cured membranes, according to the following equation:

$$\text{Conversion degree} = \left(1 - \frac{\left(\frac{C=C}{C=O} \right)_{\text{cured}}}{\left(\frac{C=C}{C=O} \right)_{\text{non-cured}}} \right) \cdot 100 \quad (1)$$

with absorbance peaks for the C=C group between 800 and 820 cm^{-1} and for the C=O group between 1715 and 1735 cm^{-1} [38]. The C=O group absorbance does not alter during curing and thus serves as reference (Figure S4). It is suspected that polymer degradation can take place during the cross-linking process. However, when comparing the ATR-FTIR spectra of a membrane coupon treated with only one pulse to that of a coupon that underwent 10 pulses, no significant differences can be observed. Especially, no new peaks seem to arise, that could be attributed to degradation.

The membrane strips were cut in smaller samples and cured at different conditions. A wet, non-cured reference sample was kept in aluminum foil until ATR-FTIR screening. As the SR399LV cross-linker has 5 reactive groups, a conversion degree of minimal 40% was considered to be a minimal requirement for successful reaction. Two reacted groups per acrylate monomer would theoretically result in an infinitely long linear polymer. As relatively short acrylate chains are anticipated, such 40 % conversion degree would theoretically also include several monomers with triple reaction i.e. forming a cross-link.

2.3.2. UV/VIS spectrophotometer

The UV-VIS spectra of PhIns were measured for 3 wt% solutions in DMF at room temperature on an Agilent 8453 UV/VIS spectrophotometer in the range of 190-1100nm. A quartz cell of 10 mm path length was used.

3. Results and discussion

3.1. Influence of storage time before UV-curing

The storage duration of polysulfone (PSU) membranes in demineralized water prior to curing clearly has a significant effect on the conversion degree (Figure 2). Membranes were either tested immediately (within hours) after phase inversion (further referred to as 'Fresh') or after more than 7 days. For the three different UV – sources, the conversion degree and thus the cross-linking efficiency is clearly lower for those samples stored for seven days prior to curing. This is most likely a consequence of the leaching and/or degradation of the photoinitiator 2,4,6-trimethylbenzoyl-diphenylphosphineoxide (TPO) during storage in demineralized water, as also observed previously [22]. In the following experiments, all membranes were cured within a few

hours after casting to ensure higher conversions. The difference in conversion degree between the three curing techniques (Figure 2) will be discussed in more detail later.

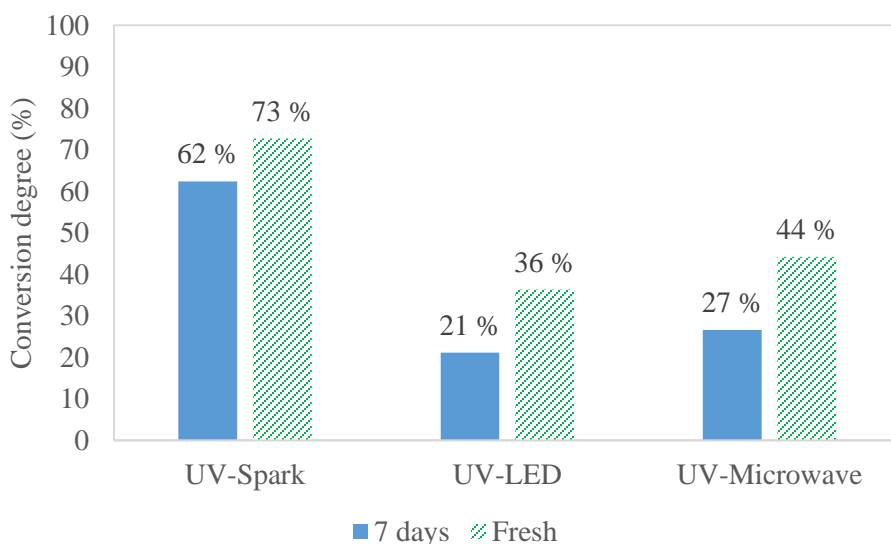


Figure 2. Conversion degree for the different UV – sources of cast films after 7 days storage in demineralized water and of the ‘Fresh’ samples.

3.2. UV - spark

For the UV – spark system, the initial selection of the parameter setting (Table 3) was based on a previous study [22], where the maximal applied energy dose was set at 12.3 J cm^{-2} . This value was thus targeted here as well by setting the energy dose to 1267 J for a curing surface of 103 cm^2 (entry 1 in Table 2). Figure 3 shows the conversion degree for several cases representing the same energy dose but either with a different number of pulses (case 1 with one pulse vs. cases 2 to 5 with 10 pulses) and/or a different pulse frequency (cases 2 to 5). An average conversion degree of 71 % was obtained. A decrease in conversion degree with an increase in the pulse frequency from 20 Hz to 1000 Hz (cases 2 to 5 in Figure 3) could be observed, explained by the effect on polymerization reaction kinetics [39]. By decreasing the time between pulses, a temperature increase takes place. This results in an increased polymerization reaction rate. On the other hand, since more radicals are present, termination reactions occur more frequently as well. Moreover, since more initiator molecules are decomposed at the beginning of the polymerization due to the higher temperature, less radicals can be formed at a later stage and the reaction might even stop because of the absence of freshly generated radicals. It is thus better to continuously have a low

concentration of radicals [39]. This results in the observed downward trend of the conversion degree with increased frequency (cases 2 to 5, Figure 3). Furthermore, when the complete energy of 12.3 J/cm² was emitted in one pulse instead of 10 pulses (case 1), a higher conversion (82 %) was achieved. Since it is known that non-transparent coatings are challenging for UV curing due to the limited penetration of light (viz. Lambert-Beer Law), longer UV irradiation or higher doses of light are required for depth curing [22,40]. This explains why increasing the energy of the UV dose results in a higher conversion degree (more depth-curing, see case 1, Figure 3). The possible effect of warmth generated by longer UV irradiation or higher doses of light was not further studied.

Table 3. Initial parameter setting of S-2200 and identification of the cases in Figure 6.

Case in Figure 3	Number of irradiation	Voltage (V)	Energy per pulse (J)	Energy (J/ cm ²)	Duration time (μs)	Mode	Frequency (Hz)
1	1	3000	1267	12.3	1392	Short	20
2	10	2000	126.6	1.23	368	Short	20
3	10	2000	126.6	1.23	368	Micro	500
4	10	2000	126.6	1.23	368	Micro	750
5	10	2000	126.6	1.23	368	Micro	1000



Figure 3. Conversion degree for different parameter settings of the UV - spark system.

In search for the maximum conversion, the number of pulses (with an energy of 12.3 J/cm^2) was increased from 1 to 12 (Figure 4). The more pulses were applied, the higher the resulting energy dose became. As a result, a slight increase in conversion was observed until an optimum was reached after 8 pulses, reaching a conversion of 88 %. Further increasing the number of pulses (10 or 12) resulted in a decreased conversion, probably as a consequence of undesired polymer degradation [22]. Unfortunately, due to the limits of the installation (max. 50 J/cm^2 per pulse), it was practically not feasible to compare the optimum conversion achieved with 8 pulses of 12.3 J/cm^2 with one single pulse of the same energy (98.4 J/cm^2). As an alternative, the energy dose was doubled to 24.6 J/cm^2 and again 8 pulses were applied (Figure 5). Unfortunately, this resulted in a decreased conversion as the energy input was too high and the sample started to burn (visualized by small burned spots that appeared at the sample edges, Figure S5).

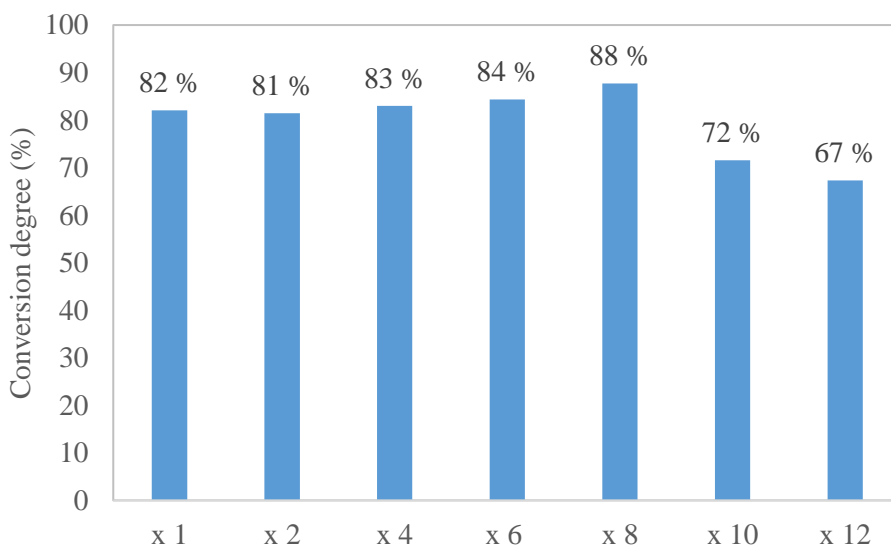


Figure 4. Influence of number of 12.3 J/cm^2 pulses on the conversion degree of the cured membrane for the UV - spark system (20 Hz).

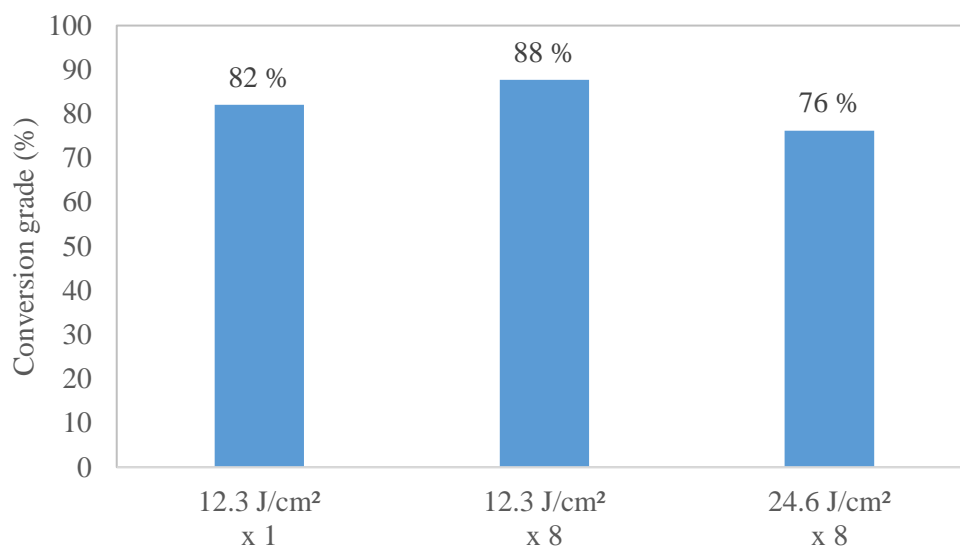


Figure 5. Influence of energy dose on the conversion degree of the cured membrane for the UV - spark system (20 Hz).

Finally, a different photo-initiator bis(2,4,6-trimethylbenzoyl)-phenylphosphineoxide (IR819) was investigated under the same test conditions. Only UV - spark and UV - LED (see section 3.4) were investigated with the alternative photo-initiator IR 819 as these are the extreme ends in terms of the spectrum range: UV - spark has a broad spectrum from 190 to 1100 nm compared to UV LED which only covers one single wavelength, i.e. 365 nm. UV - microwave lies in between them with UVA light (320 to 390 nm) as main irradiation light. It could be observed that IR 819 follows the same trend as TPO, albeit reaching lower conversions (Figure 6). This can be explained based on their respective absorbance spectra (see Figure 7), which clearly indicates a higher absorbance of light for IR 819 than for TPO [41]. This will then result in a higher amount of radicals when IR 819 is used. As a consequence, in a similar time frame, more but shorter polymers will be formed, thus resulting in a higher number of termination reactions, as mentioned before [39]. Another parameter that might influence the performance of different photo-initiators in radical polymerization is the light-induced polymerization quantum yield, Φ_p , which is the extent of how efficient the radicals are to promote the polymerization process. These values were calculated by the ratio of polymerization rate to the amount of photons absorbed by the sample. The higher this number, the more efficient the cross-linking reaction. Since this number is higher for TPO (e.g. 31.64×10^3 mol/Einstein) than for IR819 (e.g. 9.62×10^3 mol/Einstein), TPO should indeed result in higher conversions [42–47]. Influence on conversion degree due to difference in leached

amounts of photo-initiator in the coagulation bath is assumed negligible based on Hansen solubility parameter calculation [48,49].

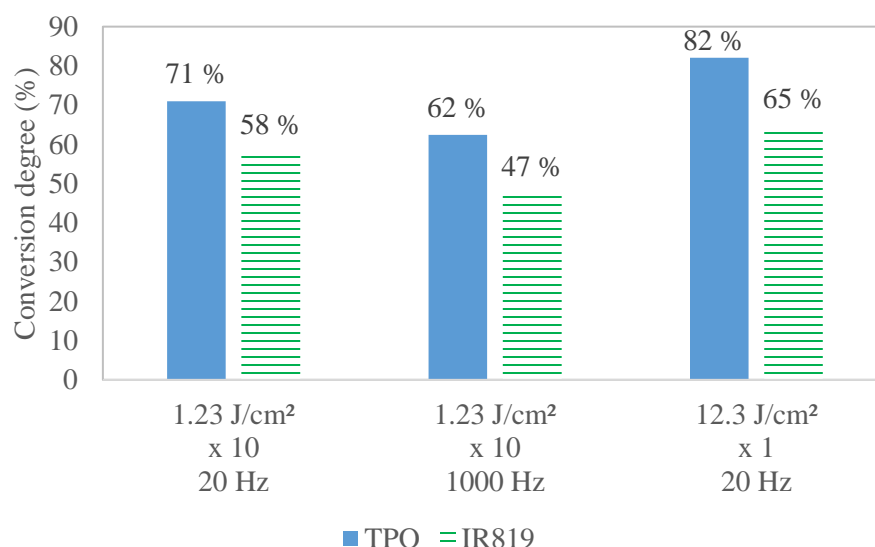


Figure 6. Comparison between the TPO and IR 819 photo-initiators with respect to the conversion degree as a function of different energy dose.

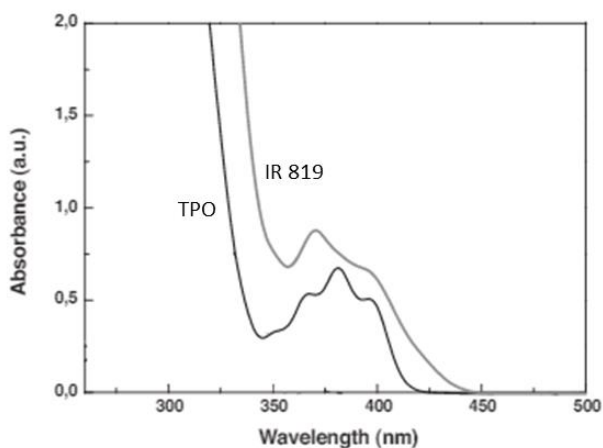


Figure 7. UV-Vis spectra of TPO, IR 819 measured under the same conditions [22].

3.3. UV - microwave

The UV - microwave unit consisted of a conveyor belt across which samples were sent for UV-curing. The samples were positioned 53 mm below the lamp with an energy of 2.26 J/cm² and a conveyor belt speed of 10 m/min. To obtain a total energy of 12.3 J/cm², the sample needed to pass 6 times through the unit. In Figure 8, an increase in the number of passages through the system does not tend to result in higher conversion. An optimum was obtained for 6 passages, in accordance with previously obtained results [22]. The conveyor belt speed was then slowed down to investigate its impact on the conversion. This resulted in higher conversions up to the point where the sample was burnt as a consequence of a too high energy dose (Figure 9). Therefore, the number of passages was set at 1 and the belt speed decreased to 1 m/min (Figure 10) to investigate a further decrease in belt speed (and thus higher energy input) without burning the sample. This resulted in higher conversions, although still lower than the optimum obtained for 6 passages at 3 m/min. This means that this setting results in the maximum energy dose that can be taken up by the sample without causing burning.

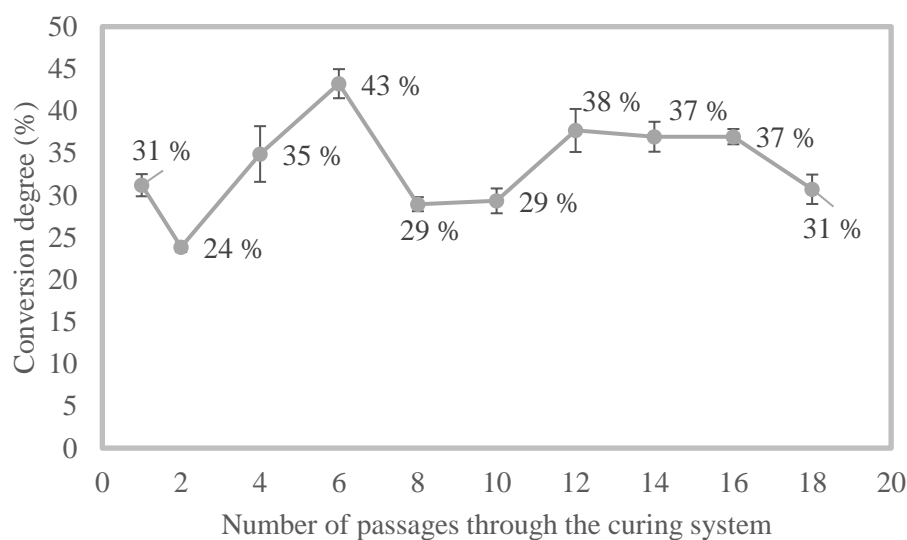


Figure 8. Conversion degree as a function of the number of passages through the UV - microwave system (12.3 J/cm², 53 mm distance and belt speed of 10 m/min).

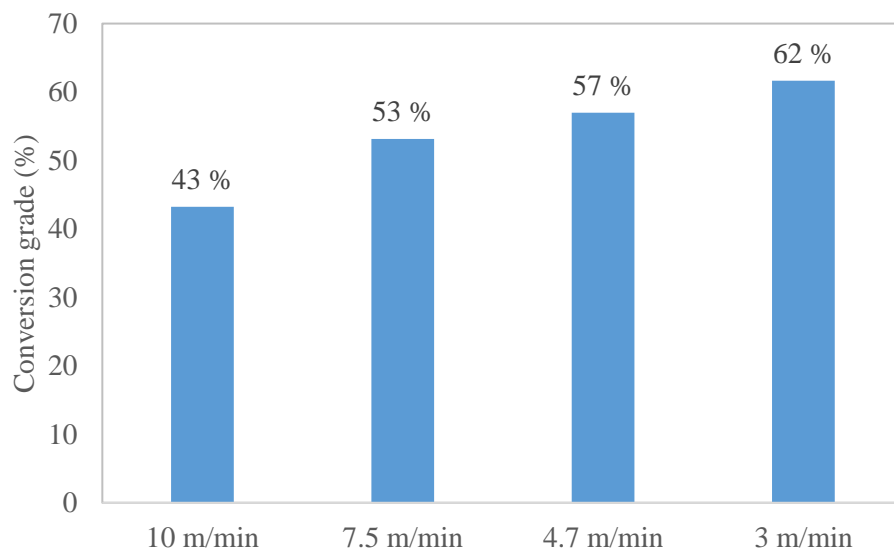


Figure 9. Conversion degree as a function of the conveyor belt speed for 6 passages. No cases available for speeds lower than 3 m/min due to sample burning.

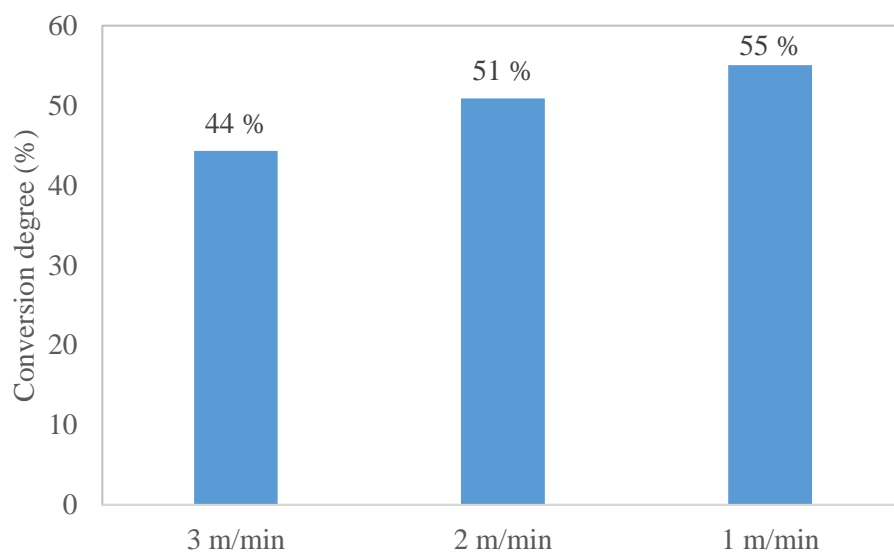


Figure 10. Conversion degree for 1 passage as a function of conversion belt speed.

3.4. UV - LED

The UV - LED curing unit was tested for the same standard membranes, investigating both photo-initiators TPO and IR 819. The samples were positioned 35 mm below the lamp, which results in an irradiance energy of 1.7 W/cm^2 . After a duration of 7 s, the energy level of 12.3 J/cm^2 could thus be obtained. No clear trend could be observed for the conversion as a function of exposure time (Figure 11), although similar trends were obtained for TPO and IR 819. It can only be tentatively concluded that a first optimum was obtained around 20 s and by further increasing the irradiance time, the conversion degree further increased. Additionally, it was discovered that delivering all the energy in one single pulse of 7 s was more efficient than irradiating the sample 10 separate times for 0.7 s (Figure 12). This could be explained by the effect of more depth-curing by the higher energy dose, as already discussed for UV - spark. However, while the type of photo-initiator had a clear impact on the conversion when using UV - spark, only a minor difference in conversion was discovered here. This is most likely caused by the fact that the wavelength of UV - LED was selected at 365 nm, which corresponds exactly with the maximum absorption of IR 819 (Figure 7). This possibly counteracts its lower quantum yield, resulting in a higher conversion for IR 819 when UV - LED was used.

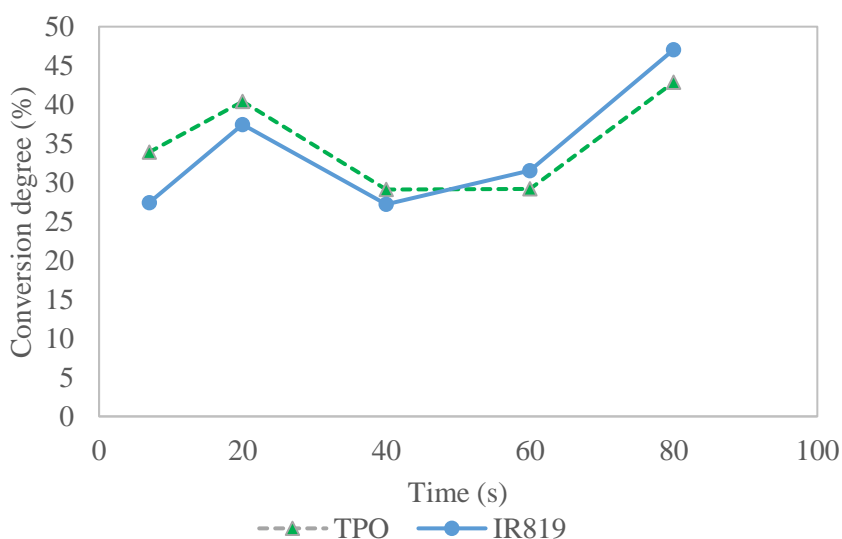


Figure 11. Conversion degree as a function of irradiance time for the UV - LED system.

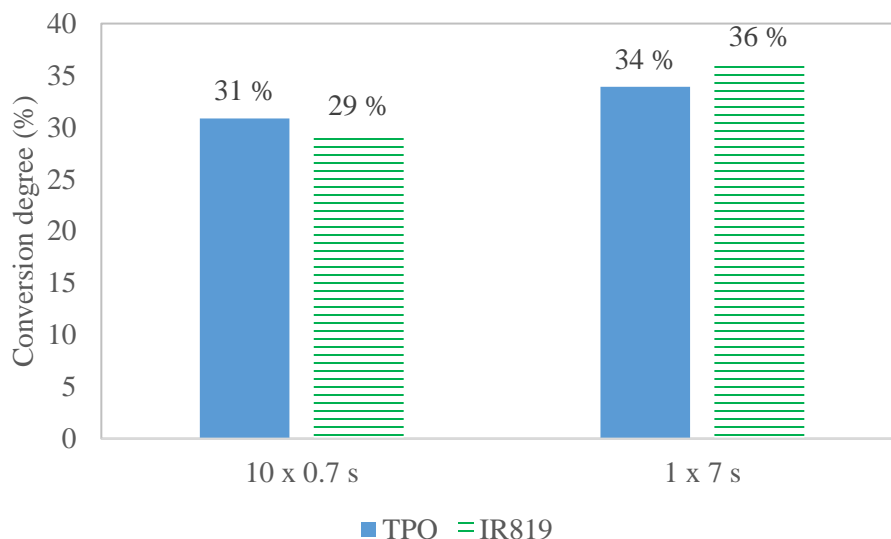


Figure 12. Difference in conversion degree between 1 pulse and 10 pulses for the UV - LED system for both photo-initiators TPO and IR 819.

For comparison of the three different UV curing systems, the maximum conversions of all three methods are summarized in Figure 13, clearly indicating that UV - spark results in the highest conversion degree (82 %) and UV - LED in the lowest (43 %).

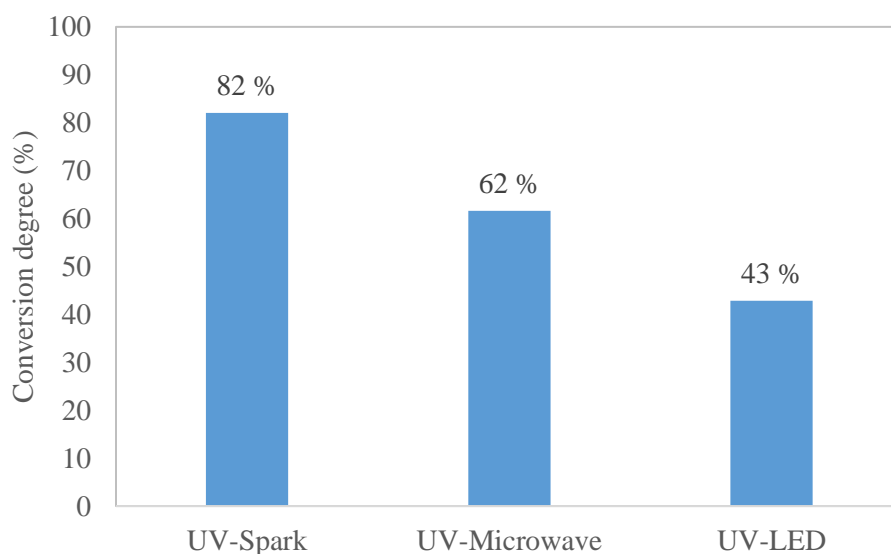


Figure 13. Maximum conversion degrees for all three UV curing systems.

The anticipated improved chemical resistance of UV cured membranes was first of all confirmed by simple visual observation after their exposure to a solvent. The chemical resistance of the PSU membrane to solvents (e.g. THF) was determined at room temperature (1) by immersion of membrane samples in THF under static conditions for 72 h, followed by solvent evaporation in an oven, and (2) by immersion in THF for 24 h while rotating (Figure 15). In method (1), the UV - LED cured membrane was clearly stable (Figure 14), while the non-cured membrane dissolved. Under dynamic conditions, the UV - LED cross-linked membranes broke in smaller fractions while the non-cured membrane dissolved completely, again evidencing the higher resistance that is obtained through curing.

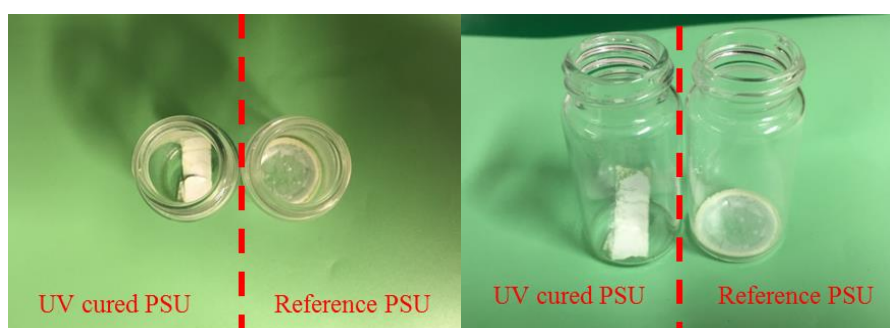


Figure 14. Solvent stability results for reference and UV – LED cured PSU membrane (80 s radiation time) after immersion in THF.

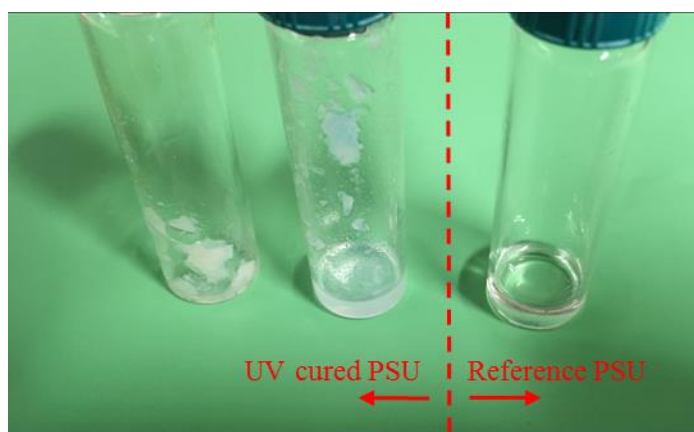


Figure 15. Solvent stability results for reference and UV - LED cured PSU membranes (both 60 s radiation time) after stirring in THF.

An additional solvent stability test was also performed by immersion at room temperature in ethyl acetate for 24 h while rotating (Figure 16). The non-cured membranes lost their structure, while UV – LED cured membranes remained as a stable film, further evidencing the higher resistance obtained through curing.



Figure 16. Solvent stability results for reference (top) and UV - LED cured (20 s radiation time) (bottom) PSU membranes after stirring in ethyl acetate.

To further prove the cross-linking realized by the UV - radiation, the residues that were obtained after method (2) were collected, washed several times and finally dried. These dried samples were analyzed with FTIR spectroscopy (Figure 17). Remaining PSU in the treated sample, i.e. either sterically or covalently captured in a cross-linked network, was evidenced by comparing its spectra with that of a PSU pellet, clearly showing overlapping peaks (especially those indicated in red). Even though hard to quantify, only a relatively low fraction of PSU seems to remain in the sample. Further investigation is thus required to optimize the chemical composition and UV curing conditions to increase this fraction.

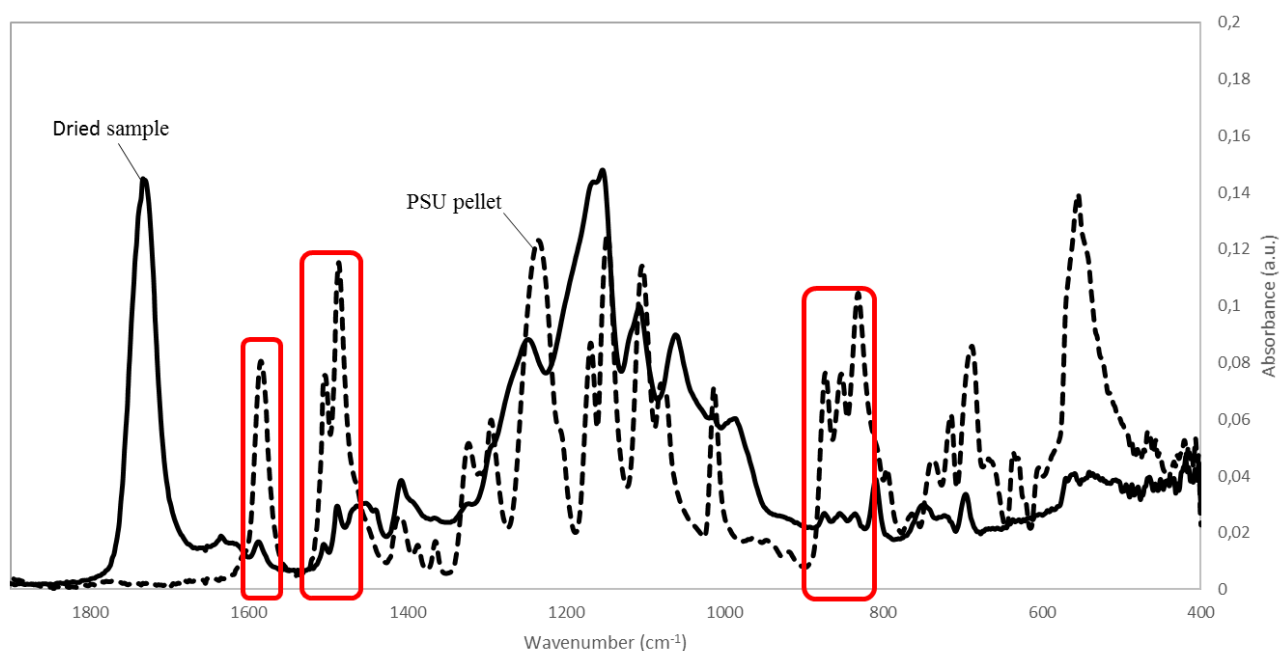


Figure 17. FTIR absorption spectra of dried sample and PSU pellet.

A final GPC-analysis was done to further prove that the obtained membranes are cross-linked (Figure 18). A sample of the solution obtained following method (2) was taken and filtered through a 0.2 μm filter before injecting it in the GPC. The peaks of all 3 components (PSU, SR399LV & TPO) from the UV cross-linked sample were lower as compared to the respective peaks from the reference uncured PSU sample. This indicates that cross-linking actually occurred during UV - radiation. As the small differences again point at a relatively low cross-linking degree, further optimization is necessary to increase the cross-linking efficiency.

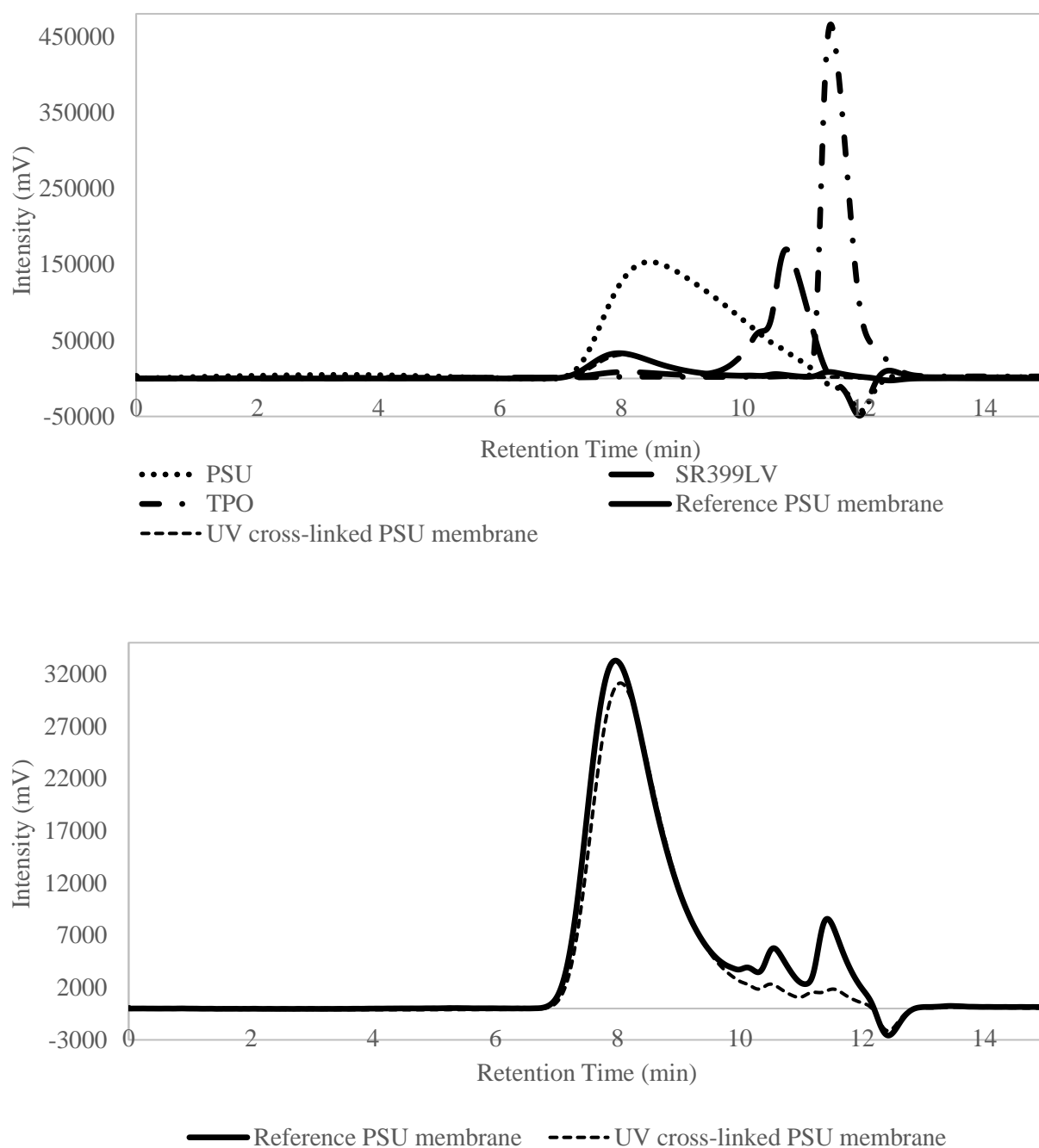


Figure 18. GPC results of (top) PSU, SR399LV, TPO and leached fraction of non-cross-linked and UV – microwave cross-linked (12 passages) sample; as well as (bottom) close-up of the latter two samples for clarification.

4. Conclusions

UV - spark proved to be the most optimal UV curing system with respect to its curing efficiency of penta-acrylates in presence of TPO or IR819 photo-initiator and its high flexibility in choice of parameter settings compared to UV - microwave and UV - LED. A too high pulse frequency had a negative influence on the conversion degree. Generally, if more tests could be done considering not only UV - light parameter settings (frequency, energy dose, distance from UV-lamp, etc.) but also compositional parameters (polymer, cross-linker and photo-initiator concentrations,...), higher curing efficiencies could probably be obtained for all three curing systems. The curing performance of the UV systems is a function of the type of photo-initiator: TPO is the best choice for UV – spark, whereas both photo-initiators TPO and IR 819 could be used with UV - LED.

Considering the important aspects for incorporating the UV curing unit in a continuous roll-to-roll system (e.g. costs, versatility, etc.), the most suitable UV curing unit could be selected. While UV - spark showed the best performance, it was not selected for further studies mainly because of its high power consumption and discontinuous mode of operation. From the remaining systems, UV - LED was selected for further studies and upscaling, even though it resulted in the lowest conversion. Nevertheless, it has a low power consumption and easily reaches the targeted minimal conversion of 40%. Although better results could be achieved with UV - microwave, it is likely that this is partly due to thermal cross-linking, which is not desirable as it simultaneously causes unwanted pore-collapse of the membranes to be prepared.

Acknowledgements

The authors acknowledge the Flemish agency for Innovation by Science and Technology (IWT) in the frame of an AIO/STW project (contract number 150474). The authors are further grateful for the financial support from the C16/17/005 funding from KU Leuven, the Belgian Federal Government through I.A.P.- P.A.I. grant (IAP 7/05 FS2). We thank Guy Koeckelberghs for the valuable discussions on the polymer chemistry. We are also grateful for the support of Polytec GmbH and UVio Ltd by providing us with the test set-up and information about the different UV units.

Data availability

The raw/ processed data required to reproduce these findings cannot be shared at this time as the data also forms part of an ongoing study

References

- [1] R. Baker, Future directions of membrane gas-separation technology, (n.d.) 6.
- [2] F.P. Cuperus, H.H. Nijhuis, Applications of membrane technology to food processing, *Trends in Food Science & Technology*. 4 (1993) 277–282. doi:10.1016/0924-2244(93)90070-Q.
- [3] D.M. Warsinger, S. Chakraborty, E.W. Tow, M.H. Plumlee, C. Bellona, S. Loutatidou, L. Karimi, A.M. Mikelonis, A. Achilli, A. Ghassemi, L.P. Padhye, S.A. Snyder, S. Curcio, C.D. Vecitis, H.A. Arafat, J.H. Lienhard, A review of polymeric membranes and processes for potable water reuse, *Progress in Polymer Science*. 81 (2018) 209–237. doi:10.1016/j.progpolymsci.2018.01.004.
- [4] D.L. Oatley-Radcliffe, M. Walters, T.J. Ainscough, P.M. Williams, A.W. Mohammad, N. Hilal, Nanofiltration membranes and processes: A review of research trends over the past decade, *Journal of Water Process Engineering*. 19 (2017) 164–171. doi:10.1016/j.jwpe.2017.07.026.
- [5] T. Wintgens, T. Melin, A. Schäfer, S. Khan, M. Muston, D. Bixio, C. Thoeye, The role of membrane processes in municipal wastewater reclamation and reuse, *Desalination*. 178 (2005) 1–11. doi:10.1016/j.desal.2004.12.014.
- [6] A. Cassano, C. Conidi, 13 - Integration of membrane technologies into conventional existing systems in the food industry, in: *Bioenergy Systems for the Future*, Woodhead Publishing, 2017: pp. 451–479. doi:10.1016/B978-0-08-101031-0.00013-2.
- [7] S. Basu, A. L. Khan, A. Cano-Odena, C. Liu, I.F. J. Vankelecom, Membrane-based technologies for biogas separations, *Chemical Society Reviews*. 39 (2010) 750–768. doi:10.1039/B817050A.
- [8] P. Vandezande, L.E. M. Gevers, I.F. J. Vankelecom, Solvent resistant nanofiltration: separating on a molecular level, *Chemical Society Reviews*. 37 (2008) 365–405. doi:10.1039/B610848M.
- [9] Y. Liu, T.-S. Chung, R. Wang, D.F. Li, M.L. Chng, Chemical Cross-Linking Modification of Polyimide/Poly(ether sulfone) Dual-Layer Hollow-Fiber Membranes for Gas Separation, *Ind. Eng. Chem. Res.* 42 (2003) 1190–1195. doi:10.1021/ie020750c.
- [10] K. Vanherck, A. Cano-Odena, G. Koeckelberghs, T. Dedroog, I. Vankelecom, A simplified diamine crosslinking method for PI nanofiltration membranes, *Journal of Membrane Science*. 353 (2010) 135–143. doi:10.1016/j.memsci.2010.02.046.
- [11] J. Mulder, *Basic Principles of Membrane Technology*, Springer Science & Business Media, 2012.
- [12] X. Chen, A Thermally Re-mendable Cross-Linked Polymeric Material, *Science*. 295 (2002) 1698–1702. doi:10.1126/science.1065879.
- [13] M.E. Rezac, E. Todd Sorensen, H.W. Beckham, Transport properties of crosslinkable polyimide blends, *Journal of Membrane Science*. 136 (1997) 249–259. doi:10.1016/S0376-7388(97)00170-1.
- [14] A.M. Kratochvil, W.J. Koros, Decarboxylation-Induced Cross-Linking of a Polyimide for Enhanced CO₂ Plasticization Resistance, *Macromolecules*. 41 (2008) 7920–7927. doi:10.1021/ma801586f.
- [15] K. Vanherck, G. Koeckelberghs, I.F.J. Vankelecom, Crosslinking polyimides for membrane applications: A review, *Progress in Polymer Science*. 38 (2013) 874–896. doi:10.1016/j.progpolymsci.2012.11.001.

- [16] X. Li, P. Vandezande, I.F.J. Vankelecom, Polypyrrole modified solvent resistant nanofiltration membranes, *Journal of Membrane Science*. 320 (2008) 143–150. doi:10.1016/j.memsci.2008.03.061.
- [17] G. Kang, Y. Cao, Application and modification of poly(vinylidene fluoride) (PVDF) membranes – A review, *Journal of Membrane Science*. 463 (2014) 145–165. doi:10.1016/j.memsci.2014.03.055.
- [18] Q. Bi, Q. Li, Y. Tian, Y. Lin, X. Wang, Hydrophilic modification of poly(vinylidene fluoride) membrane with poly(vinyl pyrrolidone) via a cross-linking reaction, *Journal of Applied Polymer Science*. 127 (n.d.) 394–401. doi:10.1002/app.37629.
- [19] A. Taguet, B. Ameduri, B. Boutevin, Crosslinking of Vinylidene Fluoride-Containing Fluoropolymers, in: *Crosslinking in Materials Science*, Springer, Berlin, Heidelberg, 2005: pp. 127–211. doi:10.1007/b136245.
- [20] A.A. Yushkin, M.N. Efimov, A.A. Vasilev, Y.G. Bogdanova, V.D. Dolzhikova, G.P. Karpacheva, A.V. Volkov, Modification of polyacrylonitrile membranes by incoherent IR radiation, *Pet. Chem.* 57 (2017) 341–346. doi:10.1134/S0965544117040089.
- [21] A.A. Yushkin, M.N. Efimov, A.A. Vasil'ev, V.I. Ivanov, Y.G. Bogdanova, V.D. Dolzhikova, G.P. Karpacheva, G.N. Bondarenko, A.V. Volkov, Effect of IR Radiation on the Properties of Polyacrylonitrile and Membranes on Its Basis, *Polym. Sci. Ser. A*. 59 (2017) 880–890. doi:10.1134/S0965545X17060104.
- [22] I. Strużyńska-Piron, J. Loccufier, L. Vanmaele, I.F.J. Vankelecom, Parameter Study on the Preparation of UV Depth-Cured Chemically Resistant Polysulfone-Based Membranes, *Macromolecular Chemistry and Physics*. 215 (2014) 614–623. doi:10.1002/macp.201300713.
- [23] Y. Liu, C. Pan, M. Ding, J. Xu, Effect of crosslinking distribution on gas permeability and permselectivity of crosslinked polyimides, *European Polymer Journal*. 35 (1999) 1739–1741. doi:10.1016/S0014-3057(98)00255-9.
- [24] V. Altun, J.-C. Remigy, I.F.J. Vankelecom, UV-cured polysulfone-based membranes: Effect of co-solvent addition and evaporation process on membrane morphology and SRNF performance, *Journal of Membrane Science*. 524 (2017) 729–737. doi:10.1016/j.memsci.2016.11.060.
- [25] S. Behnke, M. Ulbricht, Thin-film composite membranes for organophilic nanofiltration based on photo-cross-linkable polyimide, *Reactive and Functional Polymers*. 86 (2015) 233–242. doi:10.1016/j.reactfunctpolym.2014.09.027.
- [26] D. He, H. Susanto, M. Ulbricht, Photo-irradiation for preparation, modification and stimulation of polymeric membranes, *Progress in Polymer Science*. 34 (2009) 62–98. doi:10.1016/j.progpolymsci.2008.08.004.
- [27] J.S. Kang, J. Won, H.C. Park, U.Y. Kim, Y.S. Kang, Y.M. Lee, Morphology control of asymmetric membranes by UV irradiation on polyimide dope solution, *Journal of Membrane Science*. 169 (2000) 229–235. doi:10.1016/S0376-7388(99)00340-3.
- [28] J. Park, T.-H. Kim, H.J. Kim, J.-H. Choi, Y.T. Hong, Crosslinked sulfonated poly(arylene ether sulfone) membranes for fuel cell application, *International Journal of Hydrogen Energy*. 37 (2012) 2603–2613. doi:10.1016/j.ijhydene.2011.10.122.
- [29] J.G. Drobny, *Radiation Technology for Polymers*, Second Edition, CRC Press, 2010.
- [30] A.K. Hołda, I.F.J. Vankelecom, Understanding and guiding the phase inversion process for synthesis of solvent resistant nanofiltration membranes, *Journal of Applied Polymer Science*. 132 (n.d.). doi:10.1002/app.42130.

- [31] PH_HL_XEN_C-800_Brochure.pdf, (n.d.).
https://www.polytec.com/fileadmin/d/Photonik/Optische_Systeme/PH_HL_XEN_C-800_Brochure.pdf (accessed June 25, 2018).
- [32] XENON :: Pulsed Light, (n.d.). <http://www.xenoncorp.com/pulsed-light> (accessed June 25, 2018).
- [33] Heraeus Noblelight Flashlamp Catalog.pdf, (n.d.).
- [34] T.Q. Khan, P. Bodrogi, Q.T. Vinh, H. Winkler, LED Lighting: Technology and Perception, John Wiley & Sons, 2014.
- [35] F.K. Yam, Z. Hassan, Innovative advances in LED technology, *Microelectronics Journal*. 36 (2005) 129–137. doi:10.1016/j.mejo.2004.11.008.
- [36] (n.d.). <http://www.excelitas.com/Pages/Product/OmniCure-AC-8-Series.aspx> (accessed June 25, 2018).
- [37] Cary 620 FTIR Microscopes | Agilent, (n.d.).
<https://www.agilent.com/en/products/ftir/ftir-microscopes-imaging-systems/cary-620-ftir-microscopes> (accessed June 25, 2018).
- [38] Williams, Spectroscopic Meth. In Organic Chemistry, McGraw-Hill Education (India) Pvt Limited, n.d.
- [39] J.M.G. Cowie, V. Arrighi, *Polymers: Chemistry and Physics of Modern Materials*, Third Edition, CRC Press, 2007.
- [40] K. Studer, C. Decker, E. Beck, R. Schwalm, Overcoming oxygen inhibition in UV-curing of acrylate coatings by carbon dioxide inerting, Part I, *Progress in Organic Coatings*. 48 (2003) 92–100. doi:10.1016/S0300-9440(03)00120-6.
- [41] D. Nowak, J. Ortyl, I. Kamińska-Borek, K. Kukuła, M. Topa, R. Popielarz, Photopolymerization of hybrid monomers: Part I: Comparison of the performance of selected photoinitiators in cationic and free-radical polymerization of hybrid monomers, *Polymer Testing*. 64 (2017) 313–320. doi:10.1016/j.polymertesting.2017.10.020.
- [42] M.G. Neumann, C.C. Schmitt, G.C. Ferreira, I.C. Corrêa, The initiating radical yields and the efficiency of polymerization for various dental photoinitiators excited by different light curing units, *Dental Materials*. 22 (2006) 576–584. doi:10.1016/j.dental.2005.06.006.
- [43] C. Decker, Real-Time Monitoring of Polymerization Quantum Yields, 23 (1990) 4.
- [44] A.R. Shultz, Evaluation of Quantum Yields for Polymer Crosslinking and Scission by Light, *The Journal of Chemical Physics*. 29 (1958) 200–206. doi:10.1063/1.1744422.
- [45] C. Decker, Light-induced crosslinking polymerization, *Polymer International*. 51 (n.d.) 1141–1150. doi:10.1002/pi.821.
- [46] T. Scherzer, U. Decker, Real-time FTIR–ATR spectroscopy to study the kinetics of ultrafast photopolymerization reactions induced by monochromatic UV light, *Vibrational Spectroscopy*. 19 (1999) 385–398. doi:10.1016/S0924-2031(98)00070-8.
- [47] C. Decker, K. Zahouily, D. Decker, T. Nguyen, T. Viet, Performance analysis of acylphosphine oxides in photoinitiated polymerization, *Polymer*. 42 (2001) 7551–7560. doi:10.1016/S0032-3861(01)00221-X.
- [48] J. Brandrup, E.H. Immergut, E.A. Grulke, eds., *Polymer handbook*, 4th ed, Wiley, New York, 1999.
- [49] C.M. Hansen, *Hansen Solubility Parameters: A User's Handbook*, CRC Press, 2002.

List of Figures

Figure 1. Non-solvent induced phase separation (NIPS).....	5
Figure 2. Conversion degree for the different UV – sources of cast films after 7 days storage in demineralized water and of the fresh samples.	9
Figure 3. Conversion degree for different parameter settings of the UV - spark system.	10
Figure 4. Influence of number of 12.3 J/cm ² pulses on the conversion degree of the cured membrane for the UV - spark system (20 Hz).	11
Figure 5. Influence of energy dose on the conversion degree of the cured membrane for the UV - spark system (20 Hz).	12
Figure 6. Comparison between the TPO and IR 819 photo-initiators with respect to the conversion degree as a function of different energy dose.	13
Figure 7. Absorption spectra of TPO, IR 819 [12].	13
Figure 8. Conversion degree as a function of the number of passages through the UV - microwave system (12.3 J/cm ² , 53 mm distance and belt speed of 10 m/min).	14
Figure 9. Conversion degree as a function of the conveyor belt speed for 6 passages. No cases available for speeds lower than 3 m/min due to sample burning.	15
Figure 10. Conversion degree for 1 passage as a function of conversion belt speed.....	15
Figure 11. Conversion degree as a function of irradiance time for the UV - LED system.....	16
Figure 12. Difference in conversion degree between 1 pulse and 10 pulses for the UV - LED system for both photo-initiators TPO and IR 819.....	17
Figure 13. Maximum conversion degrees for all three UV curing systems.	17

List of Tables

Table 1. Chemical structure of photo-initiators and cross-linkers applied in this study.....	4
Table 2. Parameter of the UV – spark.....	6
Table 3. Initial parameter setting of S-2200 and identification of the cases in Figure 6.	10